# Distributed UAV Swarm Placement Optimization for Compressive Sensing based Target Localization

Yen-Chin Wang and Danijela Cabric
Electrical Engineering Department, University of California, Los Angeles
Email: ycwang85@ucla.edu, danijela@ee.ucla.edu

Abstract—Cooperative target localization using unmanned aerial vehicles (UAVs) swarm is gaining popularity in many applications such as disaster detection, crowd surveillance, and rescue operation. In this paper, a UAV swarm, featuring a single antenna RF transceiver per UAV, is considered and regarded as a distributed MIMO radar system for a problem of target localization. To reduce the number of measurements and computational complexity, the compressive sensing based (CS-based) algorithm is applied. In most of the existing works in radar community, the assumption of fixed radar positions is adopted. Here, by exploiting the mobility of the UAV swarm, we propose two UAV placement optimization algorithms to improve the performance of CS-based target localization. Simulation results show that compared to the random UAV placement, the mutual coherence of the measurement matrix is reduced and the localization root mean square error (RMSE) is significantly improved under the proposed UAV placement. Moreover, the RMSE performance can be further improved by increasing the number of UAVs.

Index Terms—Unmanned aerial vehicle (UAV), compressive sensing, MIMO radar, localization

### I. INTRODUCTION

Cooperative unmanned aerial vehicles (UAVs) swarm is a promising technology to detect and localize targets over large areas [1]-[3]. The target localization capability of UAV swarm plays an important role in many applications such as disaster detection, crowd surveillance, and rescue operation. In the literature, most of the works consider UAVs equipped with cameras [4][5]. However, the sensing capability of cameras suffers great degradation under bad weather or in the night. In contrast to cameras, UAV swarm equipped with RF transceivers can sense the environment day and night, regardless of the weather conditions. Moreover, since the RF transceivers are widely separated by the UAV swarm, the UAV sensing system forms a distributed multiple-input multiple-output (MIMO) radar system. It has been shown in literature [6] that the distributed MIMO radar system can improve the performance of target detection and localization by exploiting the spatial diversity of target's radar cross section (RCS). Therefore, in this paper, the UAV swarm equipped with RF transceivers is considered.

According to compressed sensing (CS) theory, a sparse signal can be reconstructed from far fewer measurements than that required in the conventional sampling theory. Therefore, if we assume that only very few targets are present in the region of interest (ROI), the CS theory can be utilized to reconstruct the scenario and localize the targets. In the literature, several CS-based localization methods for distributed MIMO radar

system have been proposed [7]-[11]. Researchers studied various design parameters to further improve the target localization performance, for example, the measurement matrix [8], the power allocation [9], and the transmitted waveforms [10]. However, since no mobile platforms are adopted in [7]-[10], all the mentioned works considered fixed antennas placement.

In this paper, CS-based target localization is adopted for UAV swarm based distributed MIMO radar. By exploiting the mobility of UAV swarm and optimizing the placement of UAVs, we reduce the mutual coherence of the dictionary matrix and improve the localization performance of CS-based method. Two algorithms are proposed to adapt UAV placement to achieve higher target localization performance. The first one is an intuitive heuristic search algorithm, and the other one is based on a gradient descent. The algorithms try to find the optimal UAV swarm placement in a given region so that the mutual coherence of the dictionary matrix is minimized. Compared to the random UAV placement, the localization root mean square error (RMSE) is significantly improved under the proposed UAV placement. Simulation results also show that under proposed UAV placement, the RMSE performance can be further improved by increasing the number of UAVs.

# II. SIGNAL AND SYSTEM MODEL

While the concepts developed for CS-based localization are quite general, for concreteness, we consider Linear Frequency Modulated Continuous Wave (LFMCW) chirp waveforms, which are one of the most widely used modulation schemes for radars because of the simplicity of hardware and signal processing. In this section, we first describe the signal model of LFMCW waveforms, and then introduce our system model.

# A. LFMCW Signal Model

In LFMCW radar, the radar transmitter radiates a continuous sinusoidal waveform whose frequency changes linearly with respect to time. The transmitted signal can be described as

$$s(t) = e^{j2\pi\phi(t)} = e^{j2\pi(f_ct + \frac{1}{2}st^2)}, \quad 0 < t \le T,$$
 (1)

where f  $_c$  is the carrier frequency, and T is the chirp duration. The frequency of s(t) is  $\frac{d\phi(t)}{dt}$  = f  $_c$  + st, which is linearly increased. The frequency modulation slope is s.

Consider a point scatter placed at a distance d from a colocated transmit and receive radar antenna. The transmitted signal is reflected back to the receive antenna from the point scatter. The received signal becomes

$$r(t) = \frac{\alpha}{d^2} s(t - \tau) = \frac{\alpha}{d^2} e^{j 2\pi (f_c(t-\tau) + \frac{1}{2} s(t-\tau)^2)},$$
 (2)

where  $\tau=2d/c$ , c is the speed of light, and  $\alpha$  is the reflectivity of the target. At the LFMCW receiver, the received signal r(t) is mixed with the transmitted s(t). The resulting signal is called intermediate frequency (IF) signal and can be expressed as

IF(t) = 
$$\frac{\alpha}{d^2} e^{j 2\pi (f_c \tau + s\tau t - \frac{1}{2}s\tau^2)}$$
. (3)

Since  $\tau$  is small,  $\frac{1}{2}s\tau^2$  in (3) can be omitted. As a result, we have

$$IF(t) = \frac{\alpha}{d^2} e^{j2\pi \frac{(f_c + st)}{c} d}.$$
 (4)

This IF signal is then used for target detection and range estimation.

## B. System Model

Given the LFMCW signal model, now we can introduce our system model where each UAV is equipped with either a LFMCW transmitter or receiver. Consider a UAV swarm of U UAVs. The number of transmitters and receivers are  $N_T$  and  $N_R$ , where  $N_R+N_T=U.$  Since one UAV can fly far away from others, the UAV swarm can be regarded as a distributed MIMO radar system and can be used to localize multiple targets. Denote the position of the mth transmitter UAV by  $p^{Tx}$   $\mathbb{P}$   $R^3$  where m  $\mathbb{P}$   $\{1,2,\ldots,N_T\}$  and the position of the nth receiver UAV by  $p^{Rx}$   $\mathbb{P}$   $R^3$  where n  $\mathbb{P}$   $\{1,2,\ldots,N_R\}.$  We assume that K targets are present in a two dimensional region of interest (ROI),  $P_{target}$  where k  $\mathbb{P}$   $\{1,2,\ldots,K\}.$ 

To simplify the design of the receiver, the transmitted signals from different transmitters are designed to be orthogonal to each other. The orthogonality can be either imposed in time or frequency domain. Let  $s_m(t)$  be the signal transmitted from the mth transmitter. The transmitted signals are reflected by the targets and captured by the receivers. The signal arriving at the nth receiver can be written as

$$r_n(t) = \sum_{m=1}^{N} \frac{\alpha_{m,n}^k}{d_{m,n,k}^2} s_m(t - \frac{d_{m,n,k}}{c})$$
 (5)

where  $\alpha_{m,n}^k$  denotes the reflectivity corresponding to the mth transmitter, nth receiver, and kth target.  $d_{m,n,k} = ||p_m^{Tx} - t_k||_2 + ||p_n^{Rx} - t_k||_2$ . It is worthwhile to note that the reflectivity is dependent on the transmitter-receiver indices. This is due to the fact that the antennas are spread widely, so the illuminated surfaces of the target from different antennas are not the same. For a co-located MIMO scenario, the reflectivity would be the same for all transmitter-recevier indices.

Under the orthogonality design of the waveforms, the signals from the mth transmitter at nth receiver can be separated and expressed as  $r_{m,n}(t) = {P \atop k=1}^{K} {\alpha_{m,n}^k \atop d_{m,n,k}^2} s_m(t-{d_{m,n,k} \atop c}) + n(t)$ , where n(t) is the additive white Gaussian (AWGN) noise. The received signal is then mixed with  $s_m(t)$  to obtain the IF signal,

and passed through the Analog-to-Digital converter (ADC) to get discrete time samples  $y_{m,n}[p]$ . As a result, we have

$$y_{m,n}[p] = \frac{\chi^{K}}{k=1} \frac{\alpha_{m,n}^{k}}{d_{m,n,k}^{2}} e^{j2\pi \frac{(f_{c}+spT_{s})}{c}d_{m,n,k}} + n[p]$$

$$= \chi^{K}$$

$$= \hat{\alpha}_{m,n}^{k} e^{j2\pi \frac{s}{c}d_{m,n,k}pT_{s}} + n[p]$$
(6)

where p and  $T_s$  denote the sampling index and the sampling interval. p = 1, 2, ..., P.

To simplify the expression of the received samples with a matrix form, we define the reflection vector  $\boldsymbol{\alpha} = [\hat{\alpha}_{1,1}^1, \hat{\alpha}_{1,2}^1, \cdots, \hat{\alpha}_{N_\top, N_R}^1, \cdots, \hat{\alpha}_{N_\top, N_R}^K]^T$  ?  $C^{N_\top N_R K},$  and the measurement matrix  $\boldsymbol{\Psi}$  with dimension  $N_T N_R P \times N_T N_R K$ , where  $\boldsymbol{\Psi} = [\Psi_1, \Psi_2, \cdots, \Psi_K],$   $\boldsymbol{\Psi}_k = [\boldsymbol{\Phi}_k(1), \boldsymbol{\Phi}_k(2), \cdots, \boldsymbol{\Phi}_k(P)]^T, \ k = 1, ..., K, \ \text{and}$ 

$$\Phi_k(p) = diag(e^{j2\pi \frac{s}{c}d_{1,1,k}pT_s}, \cdots, e^{j2\pi \frac{s}{c}d_{N_T,N_R,k}pT_s}), \quad (7)$$

where p = 1,..., P. The notation diag(e<sub>1</sub>, e<sub>2</sub>, ···, e<sub>N</sub>) denotes a diagonal matrix with diagonal elements e<sub>1</sub>, e<sub>2</sub>, ···, e<sub>N</sub>. Collecting N<sub>T</sub> N<sub>R</sub> P samples  $y_{m,n}[p]$  from all receivers and denoting  $y = [y_{1,1}[1], y_{1,2}[1], \cdots, y_{N_T, N_R}[1], \cdots, y_{N_T, N_R}[P]]^T$ , we have

$$y = \Psi \alpha + n, \qquad (8)$$

where n is the noise vector.

### III. CS-BASED TARGET LOCALIZATION METHOD

The idea of CS-based localization has been elaborated in [7]. Considering its advantages of sample reduction and great localization performance, we adopted it and applied it to our UAV swarm sensing system.

In CS-based localization, the region of interest (ROI)  $P_{target}$  is first discretized into G grid points, each of which can be regarded as a candidate of the position estimate of the target. The position of the gth grid is denoted as  $t_g^{grid}$  where g  $\boxed{2}$  {1, 2, . . . , G}. Then, the N  $_T$  N  $_R$  × G dictionary matrix  $\Psi^{grid}$  is constructed as  $\Psi^{grid}_g = [\Psi^{grid}_g, \Psi^{grid}_g, \cdots, \Psi^{grid}_g]$ , where  $\Psi^{grid}_k = [\Phi^{grid}_k(1), \Phi^{grid}_k(2), \cdots, \Phi^{grid}_k(P)]^T$ , k = 1, ..., G, and

$$\Phi_{k}^{grid}(p) = diag(e^{j2\pi \frac{s}{c}d_{1,1,k}^{grid}pT_{s}}, \cdots, e^{j2\pi \frac{s}{c}d_{N_{T},N_{R},k}^{grd}pT_{s}}), \quad (9)$$

where p = 1, ..., P and  $d_{m,n,g}^{grid} = \mathbb{P} p_m^{Tx} - t_g^{grid} \mathbb{P}_2 + \mathbb{P} p_n^{Rx} - t_g^{grid} \mathbb{P}_2$ . When K  $\mathbb{P} G$ , according to the compressed sensing theory, we can reconstruct the y in (8) with the dictionary matrix  $\Psi^{grid}$  by finding a sparse vector x. That is, a sparse vector x exists such that  $\mathbb{P} y - \Psi^{grid} x \mathbb{P}_2$  is as small as possible. Note that since  $\Psi^{grid}$  is formed by the concatenation of G diagonal matrices, each of which corresponds to one grid point in the ROI, the reconstructed x will be meaningful only if x is block-sparse. That is,  $x = [x^T, x^T, \cdots, x^T]^T$ , where g = 1, ..., G,  $x_g \mathbb{P} C^{N_T N_R}$  and only few of  $x_g$  are nonzero. Combining the above statements, the target can be localized

by solving the following CS-based optimization problem:

$$\min_{x} \ 2x \ 2_{0}$$
 s.t.  $2y - \Psi^{grid}_{x} x \ 2_{2} \le \epsilon$ ,  $x$  is block-sparse (10)

Once we acquired the block-sparse vector x, the positions of the non-zero elements in x give us the target localization estimation because each non-zero xg in x corresponds to one single grid point in the dictionary. To solve the block sparse reconstruction problem, the block orthogonal matching pursuit (BOMP) [13] is adopted in our localization.

Based on the CS theory, a dictionary with a smaller mutual coherence can guarantee a better reconstruction performance. The mutual coherence of our dictionary matrix is defined as

Since  $\Psi_i^{grid}$  is a function of transmitters' and receivers' positions, the mutual coherence is also a function of transmitters' and receivers' positions. In those previous CS-based localization works [7]-[10], the radar is fixed to the ground. However, UAV swarms are mobile. The mobility, as a newly-introduced design degree of freedom, allows us to further improve the reconstruction performance of CS-based method.

### IV. UAV PLACEMENT OPTIMIZATION

The goal is to minimize the mutual coherence by optimizing the UAV placement. In practice, the positions of UAVs are limited in a certain space S<sub>UAV</sub>. Therefore, the optimization problem can be formulated as

Solving the optimization in (12) is very difficult. Instead, we propose two algorithms, Heuristic search (HS) and Gradient descent (GD), to find the suboptimal solution.

### A. Heuristic Search (HS) placement optimization

The UAV space S<sub>UAV</sub> is uniformly discretized into Q separate grid points. Every grid point is regarded as a candidate of the UAV postion and saved in the set Sq. Then, a simple iterative search method is adopted to find the suboptimal solution of (12). At every iteration, each transmitter/receiver searches and tries all the possible grids in SQ and chooses the one which minimizes the objective function in (11). The iterative HS algorithm is summarized in the following pseudo-code:

1) Initialization:

Construct the set 
$$S_Q$$
. Then initialize  $\hat{P}^{(0)} = [p_1^{Tx}, \cdots, p_{N_T}^{Tx}, p_1^{Rx}, \cdots, p_{N_R}^{Rx}] = [\hat{p}_1^{(0)}, \dots, \hat{p}_{N_T + N_R}^{(0)}]$ .  
2) Iteration ( $N_{it}$  is the number of iteration):

For  $i = 1, 2, ..., N_{it}$  do the following.

For  $k = 1, 2, ..., N_T + N_R$ , do the following.

(i) let 
$$\hat{P}_{k}^{(i)}(w) = [\hat{p}_{1}^{(i)}, \hat{p}_{2}^{(i)}, \dots, \hat{p}_{k-1}^{(i)}, w, \hat{p}_{k+1}^{(i-1)}, \hat{p}_{k+2}^{(i-1)}, \dots, \hat{p}_{N_{T}+N_{R}}^{(i-1)}]^{T}$$
.  
(ii) Find  $\hat{w} = \arg \min_{w \in S_{R}} \mu(\Psi^{grid})$ .

(iii) Update  $\hat{p}_{k}^{(i)} = \hat{w}$ .

End For

End For

# B. Gradient Descent (GD) based Placement Optimization

In GD based placement algorithm, the iterative structure is the same as that of HS placement algorithm. The difference is that instead of searching the whole set S Q for each transmitter/receiver, we calculate the gradient of  $\mu(\Psi^{grid})$  with respect 

$$\mathbb{P}_{p^{T_{x}}}\mu(\Psi^{grid}) = \max_{\substack{i=j \\ n,p}} \frac{x}{c} \frac{4\pi s T_{s}}{c} - \mathbb{P} \mathbb{P}_{[a]} (\Psi^{grid}_{i})^{H} \Psi^{grid}_{j} \mathbb{P}_{F} p sin(a) \\
+ \mathbb{P}_{[a]} (\Psi^{grid}_{i})^{H} \Psi^{grid}_{j} \mathbb{P}_{F} p cos(a) \\
\times (\frac{p^{Tx}_{m} - t_{j}}{\mathbb{P}_{p}^{Tx}_{m} - t_{j}} - \frac{p^{Tx}_{m} - t_{i}}{\mathbb{P}_{p}^{Tx}_{m} - t_{i}}), \tag{13}$$

where  $a=\frac{2\pi spT_s}{c}$  (2  $p_m^{Tx}-t_j$  2 - 2  $p_m^{Tx}-t_i$  2 + 2  $p_n^{Rx}-t_j$  2 - 2  $p_n^{Rx}-t_i$  2),  $t_i$  is the position of the ith target and  $t_j$  is the position of the jth target. Similarly, the gradient  $\mathbb{D}\mu(\Psi^{grid})$ with respect to  $p_n^{Rx}$  is computed by replacing  $p_m^{Tx}$  in (13) with

The iterative GD algorithm is listed as follows:

1) Initialization:

$$\begin{array}{ll} \text{Initialize} & \hat{P}^{(0)} & = & [p_1^{Tx}, \cdots, p_{N_T}^{Tx}, p_1^{Rx}, \cdots, p_{N_R}^{Rx}]^T & = \\ [\hat{p}_1^{(0)}, \hat{p}_2^{(0)}, \ldots, \hat{p}_{N_T + N_R}^{(0)}]^T & . \end{array}$$

For  $i = 1, 2, ..., N_{it}$  times, do the following.

For  $k = 1, 2, ..., N_T + N_R$ , do the following.

(i) Calculate 
$$\mathbb{Z}\mu = \mathbb{Z}\mu(\Psi^{grid}(P^{(i-1)}))$$
 with respect to  $\hat{p}_k^{(i-1)}$ 

(ii) Update 
$$\hat{p}_{k}^{(i)} = \hat{p}_{k}^{(i-1)} - b_{GD}^{(i)} ? \mu$$
.

End For

End For

## V. SIMULATION RESULTS

Monte-Carlo simulation is adopted to showcase the localization performance under two proposed placement optimization algorithms. The total number of Monte-Carlo simulation Mc is  $10^4$ . The ROI S<sub>target</sub> is an 1 m  $\times$  1 m 2D plane, and there are 2 targets inside it. We discretize the ROI into 10 × 10 grid

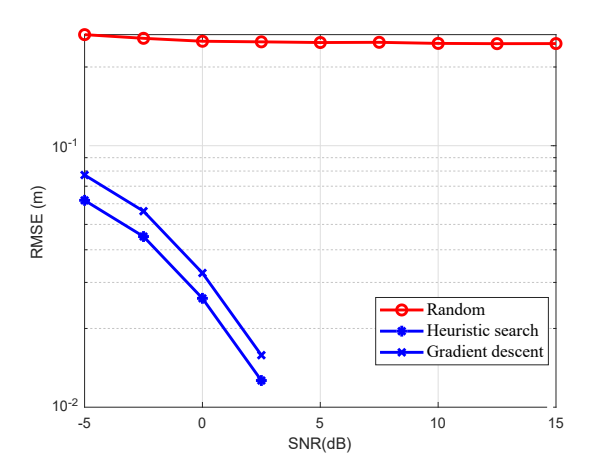


Fig. 1. The RMSE performance of 2 fixed targets, at positions [0.2 0.2], and [0.8 0.8]

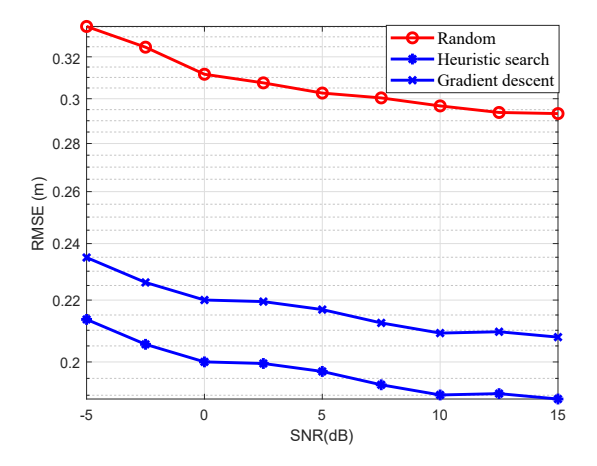


Fig. 2. The RMSE performance of 2 targets, which are randomly placed in the ROI  $\,$ 

points so that the distance between two adjacent grids is 0.1 m. The number of UAVs U is chosen from 4 to 12. The UAVs are allowed to move in a 3D space  $S_{UAV}$ , the dimension of which is 3 m  $\times$  3 m, and the location of which is 4 m above the ROI. For the LFMCW, the carrier frequency  $f_c$  is 60 GHz. The frequency modulation slope of the LFMCW signal is set to 60 MHz/ $\mu s$  and the bandwidth is 1.5 GHz. The number of samples used for processing is 256. The performance of localization is evaluated by the root mean square error (RMSE) of the estimation which is defined as

$$RMSE = \frac{\sum_{i,k} 2 t_{i} - t_{k} 2^{2}}{KMC}, \quad (14)$$

where  $\hat{t}_k^i$  is the kth target estimation in the ith Monte-Carlo trials, and  $t_k^i$  is the kth target position in the ith Monte-Carlo trials. K is the number of targets.

Fig. 1 shows the RMSE performance of the CS-based localization for 2 fixed targets under 3 different UAV placements: random placement, heuristic search placement, and gradient descent placement. 4 UAVs are considered here, with 2 of them being transmitters and 2 of them being receivers. The

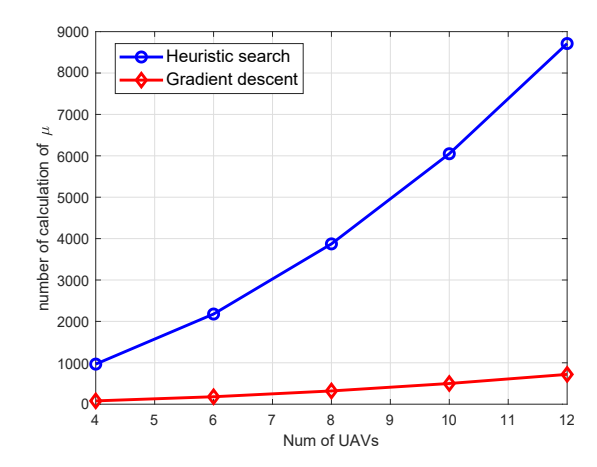


Fig. 3. Computational complexity comparison, in terms of the required number of calculation of  $\boldsymbol{\mu}$ 

targets are located at [0.2m, 0.2m] and [0.8m, 0.8m], which are exactly the grid points of our dictionary. Therefore, both proposed placements can exactly estimate the target locations at high SNR regime, while random placement cannot.

In Fig. 2, the targets are randomly placed in the entire ROI and varied across different Monte-Carlo trials. Results show that both proposed placements still outperform the random placement significantly. Here we use a big number of grid points in the search space of our heuristic search algorithm  $Q = 10^4$  such that the heuristic search placement is even slightly superior to the gradient descent placement and has the best performance.

Fig. 3 shows the comparison of the computational complexity between the two proposed algorithms. Based on the algorithm details described in Section IV, we can see that the most of the computational load for each algorithm results from the calculation of the mutual coherence (11). Therefore, we use the number of calculation of  $\mu$  as the metric for the comparison of complexity. Since the heuristic search needs to search the minimum  $\mu$  in each iteration, the number of calculation of  $\mu$  grows much faster than that of gradient descent when the number of UAVs increases.

Fig. 4 and 5 illustrate the effect of the number of the UAVs to the performance of mutual coherence and RMSE. As we can see from the figures, the more UAVs are used, the better localization performance can be achieved. This is because with more UAVs measurements, the number of rows of the dictionary matrix  $\Psi^{grid}$  becomes larger, which makes it easier for  $\Psi^{grid}$  to achieve a lower mutual coherence. As a result, after the UAV placement is carefully selected by our algorithms, the mutual coherence of  $\Psi^{grid}$  is further reduced and the RMSE performance gets improved.

In our simulation, we assume that the UAV can locate itself and move to an assigned position  $p^{Tx/Rx}$ . However, in practice, position error might occur due to the inaccuracy of the onboard sensors. When that happens, the UAV ends up stopping at position  $p^{Tx/Rx} + e_{pos}$ , instead of at  $p^{Tx/Rx}$ . Therefore, the effect of position error should be taken into consideration.

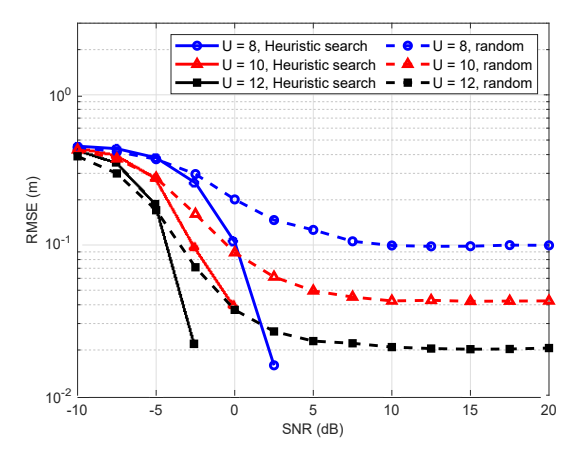


Fig. 4. The relationship between the localization performance (RMSE performance) and the number of UAVs

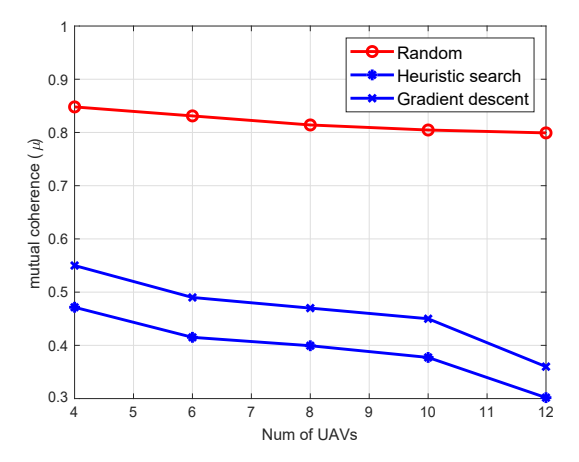


Fig. 5. The relationship between the mutual coherence of the dictionary and the number of UAVs

Fig. 6 shows the effect of the position error to the performance of mutual coherence and RMSE. The UAV swarms can have vibration which cause small position errors while they are flying in the air. The position errors are modeled as random Gaussian variables with standard deviation  $\sigma_{pos}$  and are added to all x, y, and z dimension. The number of UAVs is 8, with four transmitters and four receivers. The SNR is set to 10 dB. We can see that the performance of two proposed UAV placements outperform random placement, regardless of the value of  $\sigma_{pos}$ .

### VI. CONCLUSION

In this paper, we proposed two algorithms that optimize the placement of UAVs to improve the CS-based target localization. Based on simulation results, the UAV placements provided by both algorithms achieve much lower localization RMSE than random placement. The heuristic search based algorithm provides the best localization performance but requires higher computational resources. The gradient descent based algorithm achieves comparable performance to the heuristic search based algorithm but has lower computational complexity. The proposed placements can still provide performance

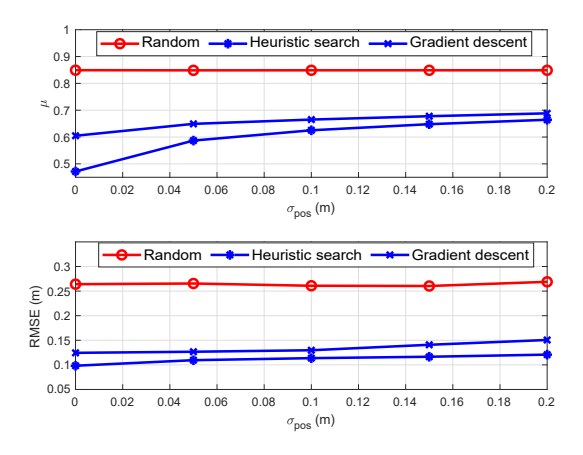


Fig. 6. The effect of the position error

improvement even with a certain degree of UAV position errors. Moreover, we show that the RMSE performance can be further improved by increasing the number of UAVs.

### REFERENCES

- [1] B. Grocholsky, J. Keller, V. Kumar and G. Pappas, "Cooperative air and ground surveillance," IEEE Robotics and Automation Magazine, vol. 13, no. 3, pp. 16-25, Sept. 2006.
- [2] X. Wang, L. T. Yang, D. Meng, M. Dong, K. Ota and H. Wang, "Multi-UAV Cooperative Localization for Marine Targets Based on Weighted Subspace Fitting in SAGIN Environment," IEEE Internet of Things Journal, vol. 9, no. 8, pp. 5708-5718, Mar. 2021
- [3] A. Guerra, N. Sparnacci, D. Dardari and P. M. Djuric, "Collabora-tive Target-Localization and Information-Based Control in Networks of UAVs," 2018 IEEE 19th International Workshop on Signal Processing Advances in Wireless Communications (SPAWC), 2018, pp. 1-5.
- [4] E. Semsch, M. Jakob, D. Pavlicek and M. Pechoucek, "Autonomous UAV Surveillance in Complex Urban Environments," 2009 IEEE/WIC/ACM International Joint Conference on Web Intelligence and Intelligent Agent Technology, Milan, Italy, 2009, pp. 82-85.
- [5] S. Minaeian, J. Liu and Y. Son, "Vision-Based Target Detection and Localization via a Team of Cooperative UAV and UGVs," IEEE Transactions on Systems, Man, and Cybernetics: Systems, vol. 46, no. 7, pp. 1005-1016, Jul. 2016.
- [6] A. M. Haimovich, R. S. Blum and L. J. Cimini, "MIMO Radar with Widely Separated Antennas," IEEE Signal Processing Magazine, vol. 25, no. 1, pp. 116-129, 2008.
- [7] Y. Yu, A. P. Petropulu and H. V. Poor, "MIMO Radar Using Compressive Sampling," IEEE Journal of Selected Topics in Signal Processing, vol. 4, no. 1, pp. 146-163, Feb. 2010.
- [8] Y. Yu, A. P. Petropulu and H. V. Poor, "Measurement Matrix Design for Compressive Sensing–Based MIMO Radar," IEEE Transactions on Signal Processing, vol. 59, no. 11, pp. 5338-5352, Nov. 2011.
- [9] Azra Abtahi, Mahmoud Modarres-Hashemi, Farokh Marvasti, Foroogh S. Tabataba, "Power allocation and measurement matrix design for block CS-based distributed MIMO radars," Aerospace Science and Technology, vol. 53, pp. 128-135, 2016,
- [10] Y. Yu, S. Sun, R. N. Madan and A. Petropulu, "Power allocation and waveform design for the compressive sensing based MIMO radar," IEEE Transactions on Aerospace and Electronic Systems, vol. 50, no. 2, pp. 898-909, 2014.
- [11] A. P. Petropulu, Y. Yu and H. V. Poor, "Distributed MIMO radar using compressive sampling," 2008 42nd Asilomar Conference on Signals, Systems and Computers, 2008, pp. 203-207.
- [12] E. J. Candes and M. B. Wakin, "An Introduction To Compressive Sampling," IEEE Signal Processing Magazine, vol. 25, no. 2, pp. 21-30, Mar. 2008.
- [13] Y. C. Eldar, P. Kuppinger and H. Bolcskei, "Block-Sparse Signals: Uncertainty Relations and Efficient Recovery," IEEE Transactions on Signal Processing, vol. 58, no. 6, pp. 3042-3054, Jun. 2010.